JACS
JOURNAL OF THE AMERICAN CHEMICAL SOCIETY
Article
pubs.acs.org/JACS

Effect of the TiO_2 Reduction State on the Catalytic CO Oxidation on Deposited Size-Selected Pt Clusters

Simon Bonanni, Kamel Aït-Mansour,* Wolfgang Harbich, and Harald Brune*

Institute of Condensed Matter Physics, Ecole Polytechnique Fédérale de Lausanne (EPFL),CH-1015 Lausanne, Switzerland

Supporting Information

ABSTRACT: The catalytic activity of deposited Pt_7 clusters has been studied as a function of the reduction state of the TiO_2(110)-(1 × 1) support for the CO oxidation reaction. While a slightly reduced support gives rise to a high catalytic activity of the adparticles, a strongly reduced one quenches the CO oxidation. This quenching is due to thermally activated diffusion of Ti^{3+} interstitials from the bulk to the surface where they deplete the oxygen adsorbed onto the clusters by the formation of TiO_x ($x \simeq 2$) structures. This reaction is more rapid than the CO oxidation. The present results are of general relevance to heterogeneous catalysis on TiO_2-supported metal clusters and for reactions involving oxygen as intermediate.

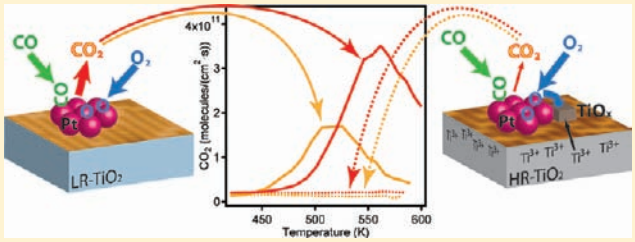

1. INTRODUCTION

In order to improve the efficiency and selectivity of modern catalysts, a detailed understanding of the interplay of the underlying physical and chemical processes is needed. This will depend on the size, composition, and morphology of the active material, and, equally importantly, on the chemical composition, morphology, and charge state of the support. Metal nanoclusters supported on well-defined single-crystal metal oxide substrates serve as model systems where these parameters can be controlled on the atomic scale.[1−20] Their catalytic properties have been studied as a function of the cluster size,[1−6] shape,[8,9] composition,[10] as well as of oxide support chemistry, surface stoichiometry,[14] and thickness.[16]

Pioneering studies by Heiz et al. have shown that the CO oxidation reaction rate over small size-selected platinum clusters supported on MgO films grown on Mo(100) is strongly influenced by the cluster size.[1] Yoon et al. have found that size-selected gold clusters adsorbed on an MgO(001) surface catalyze the CO oxidation at low temperature only in the presence of surface oxygen vacancy defects due to charging of the clusters.[14] However, on very thin MgO films (2 or 3 monolayers, ML) grown on Mo(001), catalysis of the CO oxidation by two-dimensional gold clusters has been shown to occur in the absence of the surface defects.[15,16] The two-dimensional configuration of the gold clusters has been found to be stable on 3 ML but not on 8 ML MgO films on Ag(001).[17] These studies clearly manifest the influence of the cluster-support interaction on the morphology, charge state, and catalytic activity of the clusters.

Rutile TiO_2 is one of the most studied metal oxide supports for model catalysts based on metal nanoclusters. It can be reduced by heating in vacuum creating bulk oxygen vacancies which are readily detected by the crystal changing from transparent to blue.[21] The density of bulk vacancies goes hand in hand with the one of surface vacancies, the abundance of which is therefore a measure of the bulk reduction state.[21,22] Bulk oxygen vacancies are accompanied by bulk Ti^{3+} interstitials. These are very reactive to any adsorbed oxygen once they diffuse to the subsurface region.[23,24] Recent papers by Benz et al. have shown that Ti^{3+} interstitials are responsible for breaking the CO double bond in benzaldehyde to form stilbene.[25,26] At elevated temperatures and under oxidative conditions they segregate to the surface where they form TiO_2 leading to the reoxidation of the crystal.[27−29]

It is well established that if TiO_2 is sufficiently reduced, supported nanoparticles of Pt, Ir, Rh, Ni, and Pd lose their H_2 and CO chemisorption capacity after annealing above 700 K[30] due to their encapsulation by a reduced titania layer.[31,32] This state is known as strong metal−support interaction (SMSI) state. It suppresses the catalytic activity of the nanoparticles, e.g., toward CO oxidation.[33]

In this work, we demonstrate the decisive role of the TiO_2(110) bulk reduction state on the catalytic CO oxidation over supported size-selected platinum clusters (Pt_7). Atomic resolution scanning tunneling microcopy (STM) images reveal the TiO_2 surface oxygen vacancies, and the formation of surface TiO_x ($x \simeq 2$) species after the reaction on strongly reduced supports. CO_2 production rates on the Pt clusters are 2 orders of magnitude higher when they are supported on a slightly reduced TiO_2 than on a strongly reduced one. The quenching of the CO oxidation on the strongly reduced support is identified as being caused by the surface segregation of Ti^{3+} insterstitials and their consumption of the adsorbed oxygen from the Pt clusters by spillover. This reoxidation of strongly reduced bulk titania is activated at 430 K and much more rapid

Received: October 20, 2011
Published: January 10, 2012

   dx.doi.org/10.1021/ja2098854 | J. Am. Chem. Soc. 2012, 134, 3445−3450

than the CO oxidation aimed for. We further show that the Pt clusters are clean on both supports and that the surface oxygen vacancies are not responsible for the difference in the catalytic activity, which highlights the importance of Ti^{3+} interstitials for the surface chemical reaction. The results are of general relevance to any catalytic reaction involving oxygen on titania-supported metal nanoclusters.

2. EXPERIMENTAL SECTION

The measurements have been performed in an ultrahigh vacuum (UHV, $p_{tot} \leq 1 \times 10^{-10}$ mbar) chamber combining size-selected cluster deposition, low-temperature STM,[34] and catalytic activity measurements with a highly sensitive detector.[35]

The TiO_2(110) surfaces have been prepared in UHV by repeated sputtering-annealing cycles. Oxygen is preferentially removed from the crystal leading to a TiO_{2-x} stoichiometry ($0<x<<1$). This induces the formation of defects such as surface oxygen vacancies (O_{vac}), bulk oxygen vacancies, and bulk interstitial Ti^{3+} atoms.[21,36,37] The bulk defects give rise to color centers. Increasing their concentration changes the crystal color from transparent for a perfectly stoichiometric crystal to pale yellow, light blue, dark blue, and finally black, with increasing reduction of the crystal.[21] TiO_{2-x} with $x > 1 \times 10^{-3}$ results in a black crystal with shear plane lattice defects.[28] From two initially perfectly stoichiometric TiO_2 crystals (MTI Corporation), one was transformed into a low reduction state (LR-TiO_2) and the other into a high reduction state (HR-TiO_2). The LR-TiO_2 had blue color and was prepared by 8 cycles of Ar^+ sputtering (1 kV, 1.3 μA, 13 h) and annealing at 900 K for 1 h, while the HR-TiO_2 was black and resulted from a hundred cycles of Ar^+ sputtering (1 kV, 1.3 μA, 13 h) and annealing at 1100 K for 1 h. The surface reduction states of both crystals have been determined by counting the O_{vac} densities from atomic resolution STM images.

Pt_7 clusters were deposited with a kinetic energy of 7 eV/atom on both crystal surfaces at room temperature with a density of 2×10^{-2} clusters per TiO_2(110)-(1 × 1) unit cell corresponding to a Pt coverage of 5% ML, where 1 ML is defined as the atomic density of Pt(111) (1.5×10^{15} atoms/cm^2). The Pt_7^+ current density during deposition was 1.6 ± 0.1 nA/cm^2 leading to a deposition time of 18 ± 1 min.

The CO oxidation rate has been determined by measuring the CO_2 signal as a function of sample temperature raised at a rate of 1 K/s from 300 to 600 K. The reactants O_2 and CO have been pulsed alternatingly with a delay of 5 s during this temperature ramp.[35] To distinguish the product from CO_2 in the residual gas, we have dosed $^{13}C^{16}O$ and $^{18}O_2$ and detected the yield of $^{13}C^{16}O^{18}O$. Each CO pulse corresponds to an exposure of 0.1 Langmuir (L, 1 $L = 1.33 \times 10^{-6}$ mbar · 1 s) and each oxygen pulse to 0.6 L. The CO oxidation activity of the Pt/HR-TiO_2 sample has also been measured by exposing it to a constant O_2 pressure (2.8×10^{-6}mbar) and pulsing CO (0.1 L) every 10 s. Thermal desorption spectroscopy (TDS) of CO has been performed after the CO oxidation measurement by exposing the samples to 60 L of CO at 100 K, and subsequently increasing the temperature up to 600 K at a rate of 1 K/s. The atomic scale morphologies of the pristine TiO_2(110)-(1 × 1) surfaces and of the ones with Pt_7 clusters before and after the reaction have been measured by STM at 80 K. The STM images have been recorded in the constant-current mode; the tunnel voltages given in the figure captions refer to the sample potential. The STM tips have been electrochemically etched from a tungsten wire. The WSxM software[38] has been used to process the STM images.

3. RESULTS AND DISCUSSION

Figure 1(a,b) shows STM images of the clean LR-TiO_2(110)-(1 × 1) surface. This surface exhibits small terraces with an average size of 5 nm as determined from large scale images such as Figure S2a in Supporting Information, (SI). The close-up STM image reveals the typical TiO_2(110)-(1 × 1) empty state pattern whose contrast is inverted with respect to the atomic

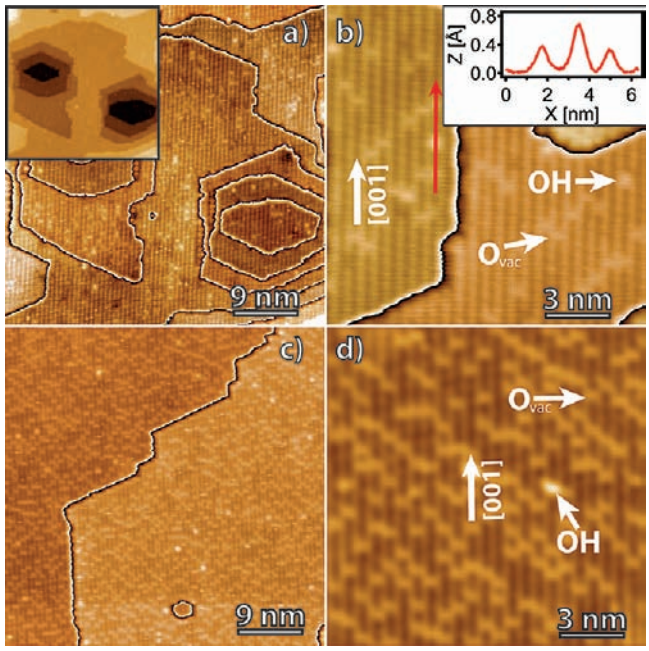

Figure 1. STM images of the clean LR (a,b) and HR (c,d) -TiO_2(110)-(1 × 1) surfaces (+1.5 V, 0.1 nA, 80 K). In (a–d), the color scale has been applied to each terrace in order to enhance the contrast. Inset in (a) shows the same as (a) with a color code revealing the terrace heights. Inset in (b), the height profile along the red arrow indicated in (b) shows the apparent heights of three point defects, two O_{vac} and one OH in between.

structure, i.e., the bright and dark lines are attributed to the [001]-oriented 5-fold-coordinated titanium atoms and protruding bridging oxygen atoms, respectively.[21] It also reveals the presence of two types of surface point defects, O_{vac} and hydroxyls (OH), which can be discerned by their apparent heights of 0.3 and 0.7 Å, respectively (see the height profile in the inset in (b)). The O_{vac} density on the surface serves as a measure of the reduction state of the crystal,[23] and amounts to 3.4% ML (two OH are considered as one O_{vac}[39−41]), where 1 ML is defined as the density of the TiO_2(110)-(1 × 1) unit cells (5.2×10^{14} cm^{-2}). Comparing this O_{vac} concentration with reported values,[21,36,37,42] we conclude that the crystal is slightly reduced. The STM images of the clean (110)-(1 × 1) surface of the HR-TiO_2 are shown in Figure 1(c,d). This surface exhibits much larger terraces (we determine a mean terrace width of 30 nm from Figure S2b of the SI), and a considerably higher O_{vac} concentration of 13.2% ML indicative of a strongly reduced crystal. However, the bulk stoichiometry must be TiO_{2-x} with x below 10^{-3}, since higher reductions are known to give rise to shear planes,[28] which we do not observe in STM.

After deposition of 5% ML Pt_7 on both LR- and HR-TiO_2(110) surfaces, randomly distributed clusters are seen in the STM images (Figure 2, parts a and b, respectively). They have an average apparent height of 4 Å, compatible with the apparent height of single-layer Pt clusters on this substrate,[20] and exhibit similar apparent height distributions on both surfaces (see Figure S5 of the SI). In both cases, they are located on the bare terraces as well as at steps, but just because the step density is much higher in the case of the LR-TiO_2, the cluster abundance at steps is also much higher. As can be seen in Figure 2(a,b), some clusters appear larger and/or higher, which we attribute to the coalescence of two clusters that have

dx.doi.org/10.1021/ja2098854 | J. Am. Chem. Soc. 2012, 134, 3445−3450

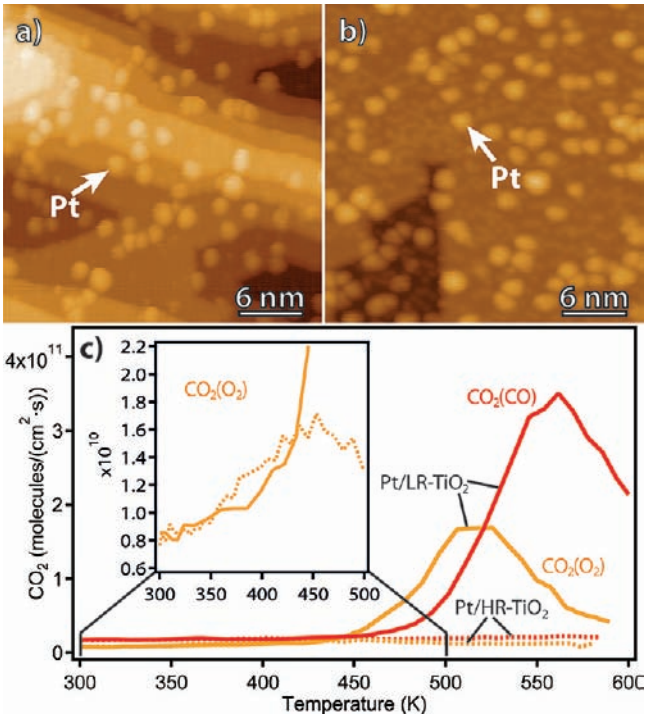

Figure 2. STM images after deposition of 5% ML Pt_7 on (a) LR- and (b) HR-TiO_2(110)-(1 × 1) (+1.5 V, 0.1 nA, 80 K). (c) CO_2 production from Pt_7/LR-TiO_2 shown as full and from Pt_7/HR-TiO_2 as dotted line. In both cases, the CO_2 correlated with the CO pulses is shown in red and the one synchronized with the O_2 pulses in orange. The inset displays a zoom of the $CO_2(O_2)$ signal from both samples between 300 and 500 K.

been deposited close by. The cluster density measured in STM is comparable with the one determined using the integral of the cluster current during the deposition. Therefore we can conclude that the clusters have a negligible surface diffusion and a mean size of 7 atoms on both TiO_2 crystals. Note that there might well be a small amount of cluster fragmentation which we cannot exclude from the observation of the mean size agreeing with the deposited one.

Figure 2c displays as full lines the CO_2 production from Pt/LR-TiO_2 measured by alternatingly pulsing CO and O_2, while the sample is annealed from 300 to 600 K. The CO_2 production synchronized with the CO pulses is displayed in red and labeled $CO_2(CO)$ and the one synchronized with the O_2 pulses in orange and labeled $CO_2(O_2)$ (see Figure S1 of the SI for the individual pulse sequences). At 300 K, we observe no CO_2 production since the Pt clusters are saturated with CO inhibiting O_2 dissociation, which is known as CO poisoning. From 360 K on, $CO_2(O_2)$ increases, indicating that CO partially desorbs from the Pt clusters leaving sites for oxygen adsorption, dissociation, and reaction with the remaining CO. The optimum balance for the applied fluxes and time delay between remaining CO and adsorbing oxygen is reached at 520 K, where the maximum of $CO_2(O_2)$ is observed. The $CO_2(CO)$ production starts to increase at 450 K and reaches its maximum at 560 K when oxygen is the dominant species on the Pt clusters so that the supplied CO can react directly with the adsorbed atomic oxygen. The observed reaction rate as function of temperature and reactants is very similar to the one of platinum single crystal surfaces.[43]

In contrast to Pt/LR-TiO_2, the CO_2 production from Pt/HR-TiO_2 displayed as dotted lines in Figure 2c, red for $CO_2(CO)$ and orange for $CO_2(O_2)$, is almost completely quenched. The inset shows that the $CO_2(O_2)$ signal on both samples increases from 360 to 430 K. However, above 430 K the $CO_2(O_2)$ production on the HR-TiO_2 surface takes on roughly a constant value, whereas the one on the LR-TiO_2 surface steeply increases. Thus, on the HR-TiO_2 sample the catalytic CO oxidation is quenched by a mechanism activated at 430 K.

After the reaction, the two samples show quite different surface morphologies as can be seen in the STM images of Figure 3(a,b). The surface of the LR-TiO_2 sample exhibits flat

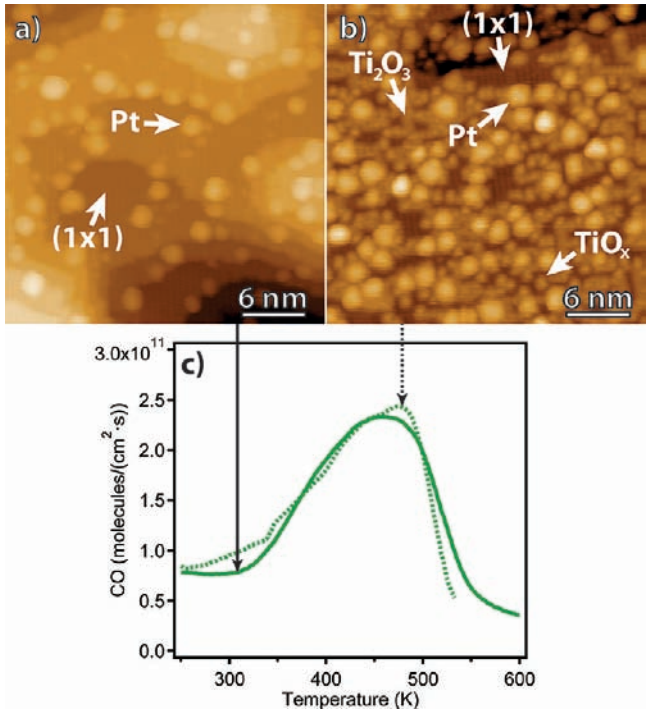

Figure 3. STM images after CO oxidation on (a) Pt/LR-TiO_2 and (b) Pt/HR-TiO_2 revealing TiO_x structures in case (b) (+1.5 V, 0.1 nA, 80 K). (c) TD spectra of CO (after adsorption of 60 L at 100 K) in solid and dotted lines from the samples shown in (a) and (b), respectively.

terraces with Pt clusters, very much as before the reaction; only the mean cluster size has increased from 7 to 10 ± 1 atoms, as inferred from the decrease of cluster density. This coarsening of the clusters is induced by the temperature rise and the exposure to gases.[44,45] The surface of the HR-TiO_2 sample exhibits after the exposure to the reactants and the temperature ramp additional structures with an apparent height of 1.9−3.2 Å coexisting with the Pt clusters appearing 6 Å high. Also on this sample the clusters coarsen; they have an average size of 11 ± 1 atoms after the reaction. We notice that the additional structures also form on the Pt-free HR-TiO_2(110) after heating to 600 K under O_2 and CO exposure (see Figure S4 of the SI). They are attributed to TiO_x species similar to those previously observed after exposure of clean reduced TiO_2(110) surfaces at elevated temperatures to oxygen, due to the oxidation of segregating Ti^{3+} interstitials.[27,46] In fact, the Ti^{3+} interstitials present in a reduced TiO_2 bulk crystal are mobile above 400 K.[47] Once they reach the subsurface region, they react with any oxygen present at the surface to form a great variety of TiO_x

dx.doi.org/10.1021/ja2098854 | J. Am. Chem. Soc. 2012, 134, 3445−3450

structures which are the manifestation of the TiO_2 reoxidation process.[27,46,47] The fact that the TiO_x structures are almost absent on the surface of the LR-TiO_2 sample is attributed to the much lower bulk concentration of Ti^{3+} interstitials in this crystal.

In order to investigate whether the Pt clusters are clean or encapsulated by a passivating titania layer,[31−33] we have performed CO TDS measurements on both samples after the reaction. These are displayed in Figure 3c as full and dotted lines, respectively. In both cases, there is a broad peak ranging from ∼350 to ∼500 K reminiscent of the desorption of CO from Pt terraces (at ∼400 K) and steps (at ∼470 K).[48,49] As expected for our case of small clusters, the CO desorption from low coordinated Pt atoms is found dominant. The two TD spectra of Figure 3c are almost identical revealing that both samples have compatible densities of Pt adsorption sites for CO, which excludes an SMSI state as a reason for the quenching of the catalytic activity on the HR-TiO_2 support.

In order to clarify whether the surface O_{vac} are the origin of the absence of catalytic activity of the HR-TiO_2 sample, we have prepared an HR-TiO_2 sample without surface O_{vac}. Exposure of this surface to 50 L of O_2 at 100 K and subsequent annealing it to 300 K heals the surface O_{vac}.[42] (For an atomic scale image of the resulting surface, see Figure S3 of the SI.) Figure 4 shows this surface after Pt_7 deposition at 300 K and

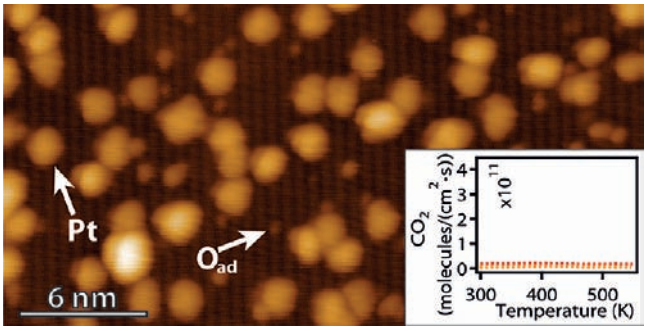

Figure 4. STM image of 5% ML Pt_7 on HR-TiO_2(110)-(1 × 1) pre-exposed to 50 L of O_2 at 100 K (+1.5 V, 0.1 nA, 80 K). Inset is the corresponding CO_2 production displayed with the same color code as in Figure 2c.

reveals that it is still bare of O_{vac}. We find that the CO_2 production from this sample is negligible (see inset in Figure 4); therefore, the surface O_{vac} are not responsible for the catalytic passivity of the HR-TiO_2-supported Pt clusters, which has hence to be solely ascribed to bulk defects.

These observations of newly created surface TiO_x features, of the cleanliness of the Pt clusters, and of the negligible role of surface O_{vac} suggest the following scenario for the HR-TiO_2 sample. On this sample, the dosed oxygen adsorbed on the Pt clusters is depleted via spillover from the clusters to the support surface where it is consumed by reaction with surface segregating Ti^{3+} interstitials (see sketch in Figure 5). Since Ti^{3+} interstitials are much more abundant in the HR-TiO_2 subsurface region than in the LR-TiO_2 one, the HR-TiO_2 surface can adsorb much more oxygen than the LR-TiO_2 one.[23,24] This explains why much more TiO_x structures are observed after the catalytic CO oxidation on Pt/HR-TiO_2 than on Pt/LR-TiO_2. The absence of CO_2 production from Pt/HR-TiO_2 indicates that Ti^{3+} interstitials react not only with the oxygen arriving from the gas phase directly at the TiO_2 surface,

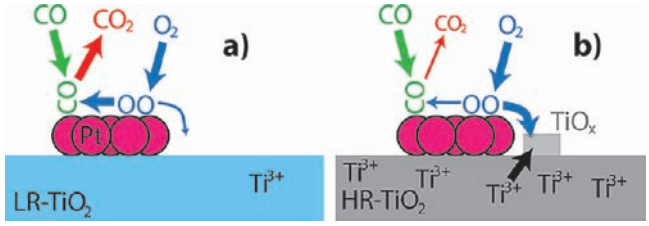

Figure 5. Schematic diagram explaining the difference in the catalytic CO oxidation activity between Pt_7/LR-TiO_2 and Pt_7/HR-TiO_2. (a) On the LR-TiO_2 sample most of the oxygen remains chemisorbed on the Pt clusters and oxidizes the dosed CO. (b) On the HR-TiO_2 sample oxygen mainly spills over and reacts with Ti^{3+} interstitials to form TiO_x on the surface, instead of reacting with the dosed CO.

but also with the oxygen adsorbed on the Pt clusters via spillover to the nearby TiO_2 surface. This reaction is more rapid and energetically more favorable than the CO oxidation since the binding energy of an oxygen atom is higher in TiO (6.87 eV[50]) and in TiO_x (3.34 eV[36]) than in CO_2 (2.94 eV[51]). This opens up an effective sink for the adsorbed oxygen which, instead of being consumed by CO to produce CO_2, is consumed by Ti^{3+} to produce TiO_x (Figure 5b). Bennet et al. have observed such an oxygen spillover for larger Pd clusters on strongly reduced TiO_2(110) above 550 K,[46] while Kaden et al. have seen no evidence for oxygen spillover up to 500 K for a sample with smaller Pd clusters adsorbed on slightly reduced TiO_2(110).[5] These observations find an explanation in the present results, i.e., oxygen spillover occurs only on strongly reduced TiO_2 and only above 400 K, where the mobility of Ti^{3+} interstitials is activated.

The model schematized in Figure 5 is further corroborated by measuring the CO_2 production rate from a freshly prepared Pt/HR-TiO_2 sample (as the one in Figure 2b) exposed to a constant O_2 pressure of 2.8 × 10^{-6} mbar corresponding to a 30 times higher dose than in the pulsed O_2 experiments. Now the CO_2 production at each CO pulse, shown as dotted line in Figure 6, is comparable to the one obtained from Pt/LR-TiO_2

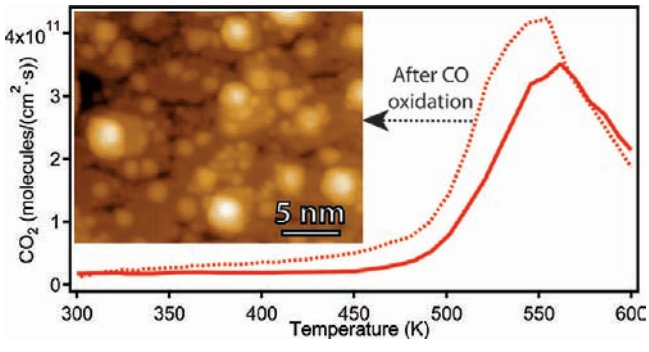

Figure 6. Dotted line, CO_2 production from Pt/HR-TiO_2 obtained by exposing the sample to a constant O_2 pressure of 2.8 × 10^{-6} mbar and pulsing CO (0.1 L per pulse). Solid line, the same as in Figure 2c, i.e., CO_2(CO) component of the CO_2 production from Pt/LR-TiO_2 obtained by alternatingly pulsing CO (0.1 L) and O_2 (0.6 L). To facilitate the comparison of the two measurements obtained with different pressure conditions, a CO_2 background of 4.9 × 10^{10} molecules/(cm^2·s) has been subtracted for the dotted line. Inset, STM image of Pt/HR-TiO_2 after the CO_2 production with the high oxygen exposure (+1.5 V, 0.1 nA, 80 K).

by alternatingly pulsing CO and O_2 shown as full line for comparison. Since oxygen is supplied at a much higher rate, the

dx.doi.org/10.1021/ja2098854 | J. Am. Chem. Soc. 2012, 134, 3445−3450

oxygen spillover mechanism is saturated and the Pt clusters can reach an oxygen coverage comparable to the one of Pt/LR-TiO_2 with 0.6 L O_2 pulses. In addition, this high O_2 exposure of Pt/HR-TiO_2 results in the growth of new complete TiO_2(110)-(1 × 1) layers beside TiO_x structures, and finally the coarsening of the Pt clusters is also enhanced, as seen in the STM image of Figure 6.

4. CONCLUSIONS

In summary, we have conducted a systematic UHV study to show the relevance of the bulk reduction state of TiO_2(110) on the catalytic CO oxidation on supported Pt_7 clusters. We have used two types of TiO_2 supports with low and high reduction (LR, HR) states revealed by their clean (110)-(1 × 1) surfaces containing 3.4% and 13.2% ML O_{vac}, respectively. Catalysis measurements performed by alternatingly pulsing CO and O_2 and simultaneously annealing the sample from 300 to 600 K show that the maximum CO_2 production rate of the Pt clusters is 2 orders of magnitude higher when they are supported on LR- than on HR-TiO_2. The quenching of the CO_2 production on Pt/HR-TiO_2 is due to the depletion of the dosed oxygen adsorbed on the Pt clusters via spillover to the support and its consumption by reaction with segregating Ti^{3+} interstitials. An SMSI state could be excluded and we demonstrated that the role of surface oxygen vacancies is negligible; they only serve as indicator of the bulk reduction state. On the basis of these results, we generally expect that the bulk reduction state of TiO_2 strongly affects the catalytic activity of supported metal clusters in chemical reactions between oxygen and other molecules.

■ ASSOCIATED CONTENT

Supporting Information

Details of the catalysis measurements and supplementary STM measurements. This material is available free of charge via the Internet at http://pubs.acs.org.

■ AUTHOR INFORMATION

Corresponding Author

harald.brune@epfl.ch; kamel.ait-mansour@epfl.ch

■ ACKNOWLEDGMENTS

Support from the Swiss National Science Foundation is gratefully acknowledged.

■ REFERENCES

(1) Heiz, U.; Sanchez, A.; Abbet, S.; Schneider, W.-D. *J. Am. Chem. Soc.* **1999**, *121*, 3214.
(2) Kaden, W. E.; Wu, T.; Kunkel, W. A.; Anderson, S. L. *Science* **2009**, *326*, 826.
(3) Valden, M.; Lai, X.; Goodman, D. W. *Science* **1998**, *281*, 1647.
(4) Lee, S.; Fan, C.; Wu, T.; Anderson, S. L. *J. Am. Chem. Soc.* **2004**, *126*, 5682.
(5) Kaden, W. E.; Kunkel, W. A.; Kane, M. D.; Roberts, F. S.; Anderson, S. L. *J. Am. Chem. Soc.* **2010**, *132*, 13097.
(6) Wu, T.; Kaden, W. E.; Kunkel, W. A.; Anderson, S. L. *Surf. Sci.* **2009**, *603*, 2764.
(7) Ortiz-Soto, L. B.; Alexeev, O. S.; Amiridis, M. D. *Langmuir* **2006**, *22*, 3112.
(8) Paredis, K.; Ono, L. K.; Mostafa, S.; Li, L.; Zhang, Z.; Yang, J. C.; Barrio, L.; Frenkel, A. I.; Roldan Cuenya, B. *J. Am. Chem. Soc.* **2011**, *133*, 6728.
(9) Mostafa, S.; Behafarid, F.; Croy, J. R.; Ono, L. K.; Li, L.; Yang, J. C.; Frenkel, A. I.; Roldan Cuenya, B. *J. Am. Chem. Soc.* **2010**, *132*, 15714.
(10) Mott, D.; Luo, J.; Njoki, P. N.; Lin, Y.; Wang, L.; Zhong, C.-J. *Cat. Today* **2007**, *122*, 378.
(11) Libuda, J.; Freund, H.-J. *Surf. Sci. Rep.* **2005**, *57*, 157.
(12) Sun, Y.-N.; Qin, Z.-H.; Lewandowski, M.; Kaya, S.; Shaikhutdinov, S.; Freund, H.-J. *Catal. Lett.* **2008**, *126*, 31.
(13) Ono, L. K.; Yuan, B.; Heinrich, H.; Roldan Cuenya, B. *J. Phys. Chem. C* **2010**, *114*, 22119.
(14) Yoon, B.; Häkkinen, H.; Landman, U.; Wörz, A. S.; Antonietti, J. M.; Abbet, S.; Judai, K.; Heiz, U. *Science* **2005**, *307*, 403.
(15) Zhang, C.; Yoon, B.; Landman, U. *J. Am. Chem. Soc.* **2007**, *129*, 2228.
(16) Harding, C.; Habibpour, V.; Kunz, S.; Farnbacher, A. N.-S.; Heiz, U.; Yoon, B.; Landman, U. *J. Am. Chem. Soc.* **2009**, *131*, 538.
(17) Sterrer, M.; Risse, T.; Heyde, M.; Rust, H.-P.; Freund, H.-J. *Phys. Rev. Lett.* **2007**, *98*, 206103.
(18) Tong, X.; Benz, L.; Kemper, P.; Metiu, H.; Bowers, M. T.; Buratto, S. K. *J. Am. Chem. Soc.* **2005**, *127*, 13516.
(19) Kaden, W. E.; Kunkel, W. A.; Anderson, S. L. *J. Chem. Phys.* **2009**, *131*, 114701.
(20) Isomura, N.; Wu, X.; Watanabe, Y. *J. Chem. Phys.* **2009**, *131*, 164707.
(21) Diebold, U. *Surf. Sci. Rep.* **2003**, *48*, 53.
(22) Pang, C. L.; Lindsay, R.; Thornton, G. *Chem. Soc. Rev.* **2008**, *37*, 2328.
(23) Lira, E.; Hansen, J. Ø.; Huo, P.; Bechstein, R.; Galliker, P.; Lægsgaard, E.; Hammer, B.; Wendt, S.; Besebacher, F. *Surf. Sci.* **2010**, *604*, 1945.
(24) Lira, E.; Wendt, S.; Huo, P.; Hansen, J. Ø.; Streber, R.; Porsgaard, S.; Wei, Y.; Bechstein, R.; Lægsgaard, E.; Besenbacher, F. *J. Am. Chem. Soc.* **2011**, *133*, 6529.
(25) Benz, L.; Haubrich, J.; Quiller, R. G.; Jensen, S. C.; Friend, C. M. *J. Am. Chem. Soc.* **2009**, *131*, 15026.
(26) Benz, L.; Haubrich, J.; Jensen, S. C.; Friend, C. M. *ACS Nano* **2011**, *5*, 834.
(27) Onishi, H.; Iwasawa, Y. *Phys. Rev. Lett.* **1996**, *76*, 791.
(28) Bennett, R. A. *PhysChemComm* **2000**, *3*, 9.
(29) Bowker, M.; Bennett, R. *J. Phys.: Condens. Matter* **2009**, *21*, 474224.
(30) Tauster, S. J.; Fung, S. C.; Garten, R. L. *J. Am. Chem. Soc.* **1978**, *100*, 170.
(31) Tauster, S. J. *Acc. Chem. Res.* **1987**, *20*, 389.
(32) Dulub, O.; Hebenstreit, W.; Diebold, U. *Phys. Rev. Lett.* **2000**, *84*, 3646.
(33) Bonanni, S.; Aït-Mansour, K.; Brune, H.; Harbich, W. *ACS Catal.* **2011**, *1*, 385.
(34) Jödicke, H.; Schaub, R.; Bhowmick, A.; Monot, R.; Buttet, J.; Harbich, W. *Rev. Sci. Instrum.* **2000**, *71*, 2818.
(35) Bonanni, S.; Aït-Mansour, K.; Hugentobler, M.; Brune, H.; Harbich, W. *Eur. Phys. J. D* **2011**, *63*, 241.
(36) Wendt, S.; Sprunger, P. T.; Lira, E.; Madsen, G. K. H.; Li, Z.; Hansen, J. Ø.; Matthiesen, J.; Blekinge-Rasmussen, A.; Lægsgaard, E.; Hammer, B.; Besenbacher, F. *Science* **2008**, *320*, 1755.
(37) Yim, C. M.; Pang, C. L.; Thornton, G. *Phys. Rev. Lett.* **2010**, *104*, 036806.
(38) Horcas, I.; Fernández, R.; Gómez-Rodríguez, J. M.; Colchero, J.; Gómez-Herrero, J.; Baro, A. M. *Rev. Sci. Instrum.* **2007**, *78*, 013705.
(39) Zhang, Z.; Bondarchuk, O.; Kay, B. D.; White, J. M.; Dohnálek, Z. *J. Phys. Chem . B* **2006**, *110*, 21840.
(40) Wendt, S.; Schaub, R.; Matthiesen, J.; Vestergaard, E. K.; Wahlström, E.; Rasmussen, M. D.; Thostrup, P.; Molina, L. M.; Lægsgaard, E.; Stensgaard, I.; Hammer, B.; Besenbacher, F. *Surf. Sci.* **2005**, *598*, 226.
(41) Li, S.-C.; Zhang, Z.; Sheppard, D.; Kay, B. D.; White, J. M.; Du, Y.; Lyubinetsky, I.; Henkelman, G.; Dohnálek, Z. *J. Am. Chem. Soc.* **2008**, *130*, 9080.

(42) Zhang, Z.; Lee, J.; Yates, J. T. Jr.; Bechstein, R.; Lira, E.; Hansen, J. Ø.; Wendt, S.; Besenbacher, F. *J. Phys. Chem. C* **2010**, *114*, 3059.
(43) Campbell, C. T.; Ertl, G.; Kuipers, H.; Segner, J. *J. Chem. Phys.* **1980**, *73*, 5862.
(44) Simonsen, S. B.; Chorkendorf, I.; Dahl, S.; Skoglundh, M.; Sehested, J.; Helveg, S. *J. Am. Chem. Soc.* **2010**, *132*, 7968.
(45) Tao, F.; Dag, S.; Wang, L.-W.; Liu, Z.; Butcher, D. R.; Bluhm, H.; Salmeron, M.; Somorjai, G. A. *Science* **2010**, *327*, 850.
(46) Bennett, R. A.; Stone, P.; Bowker, M. *Catal. Lett.* **1999**, *59*, 99.
(47) Stone, P.; Bennett, R. A.; Bowker, M. *New J. Phys.* **1999**, *1*, 8.
(48) Qin, Z.-H.; Lewandowski, M.; Sun, Y.-N.; Shaikhutdinov, S.; Freund, H.-J. *J. Phys. Chem. C* **2008**, *112*, 10209.
(49) Lundwall, M. J.; McClure, S. M.; Goodman, D. W. *J. Phys. Chem. C* **2010**, *114*, 7904.
(50) Loock, H.-P.; Simard, B.; Wallin, S.; Linton, C. *J. Chem. Phys.* **1998**, *109*, 8980.
(51) Yeo, Y. Y.; Vattuone, L.; King, D. A. *J. Chem. Phys.* **1997**, *106*, 392.